Development of chitosan base $PbBiS_2$ thin films for photovoltaic application

D. Shanthi[a], A. Yogananth[b], S. Anandhavelu[c*], V. Balasubramanian[d], J. Suresh[e], S. A. Babu[c], S. Sarveswaran[f]

[a]*Department of Chemistry, Vel Tech Multi Tech Dr.Rangarajan Dr.Sakunthala Engineering College, Avadi, Tamilnadu, India.*

[b]*Department of Chemistry, Sanghamam College of Arts and Science, Melmalyanur, Tamilnadu, India.*

[c]*Department of Applied Chemistry, Sri Venkateswara College of Engineering, Pennalur, Sriperumbudur-602117,Tamilnadu, India.*

[d]*Department of Science, Amrita Vidyalayam, Nallampalayam, Coimbatore 641 006, Tamil Nadu, India.*

[e]*Department of Chemistry, Sri Ramakrishna Engineering College, N.G.G.O Colony, Coimbatore-641 022, Tamilnadu, India.*

[f]*Department of Robotics and Automation, Sri Ramakrishna Engineering College, Coimbatore-641 022, Tamilnadu, India.*

Novel poly-crystalline nature of chitosan (CS) based Lead Bismuth Sulphide (PbBiS2) thin films have been deposited at different deposition temperatures by chemical bath deposition (CBD), a lucid and low cost technique. Structural, optical and electrical properties of the films were investigated using X-ray diffraction (XRD), Energy dispersive analysis of X-ray (EDAX), Scanning Electron Microscopy (SEM), Spectrophotometry, Photoluminescence, Hall Effect and Current-Voltage (I-V) estimations. The films were identified to be polycrystalline with orthorhombic shape. The films exhibited a highly reflective surface with a metal appearance. The optical band differences on the films ranged from 2.22 to 1.97 eV. The negative nature of the Hall coefficients indicated that the majority of load-carrying materials were electrons. The intensity of the photo-luminescence emission was increased. Current-voltage measurements reported the semiconductor nature of the film. The prepared thin films are suitable for solar cell applications.

(Received July 16, 2022; Accepted October 14, 2022)

Keywords: Thin films, Chemical bath deposition, $PbBiS_2$, SEM, PL, I-V measurement

1. Introduction

The bismuth preferably rhombohedral crystal with ideal quality portrayed as semiconductor film materials are reliable in the center due to their outstanding structural, electronic and optical properties. Recent all-embracing research has been dedicated to the development of various kinds of binary and ternary layers of semiconductor thin films like Monovalent silver cations incorporated on bismuth-based thin-film for the production of enhanced photovoltaic absorbers which shows excellent stability over at least 10 days under ambient conditions. Grapheme thin films make use of highly conducting and transparent electrodes in flexible, stretchable, foldable electronics. And, InGaN nanowire white-emitting planar LEDs have been fabricated to achieve quantum confined Stark effect [1-4].

Bismuth chalcogenides, for instance, Bi_2S_3, BiSe, CuBiS, $CsBi_4Te_6$ indicates fascinating non-linear optical characteristics far beyond the second harmonic effect [5-6]. Bismuth Triiodide as a contender thin-film photovoltaic absorber has established for its optical properties and the potential for "defect-tolerant" charge drift properties, which proved by measuring optical absorption and recombination lifetimes. BiI_3 thin films were prepared by physical vapor transport,

* Corresponding authors: sranand2204@gmail.com
https://doi.org/10.15251/CL.2022.1910.725

solution processing and single-crystals by an electrodynamic gradient vertical Bridgman method. Various micro and nano structures of the Bismuth-containing compound have been composed, manufactured and characterized in the previous decades for their potential applications in photo voltaic enterprises [7-9].

Metal doped metal oxide thin films were prepared on glass substrate by spray pyrolysis technique, magnetron sputtering at room temperature, chemical controlling deposition bath, molecular beam epitaxy, dip-coating, spin-coating, sol-gel method, vacuum filtration, electrophoretic deposition, pulse electro deposition, chemical vapor deposition and layer-by-layer self assembly [10-16]. Among these techniques, chemical bath deposition technique is quite simple, quick, economical, easily covering of giant area surfaces and without much of a stretch be connected to an industrial scale which has very intrigue to other process. Single-crystalline lead bismuth sulphide thin films were successfully deposited on glass substrate by chemical bath deposition technique is a promising candidate for photovoltaic device applications. Thin film growth can take place by ion-by-ion condensation of the materials on the substrates by adsorption of colloidal particles from the solution on the substrate [17-18].

Various form of thin films prepared like flexible or rigid, metal or insulator that can be used for improved storage device performance. Ga-doped ZnO thin films proved as transparent electrodes in photovoltaic cells. Lead chalcogenides including Lead sulfide (Pbs), Lead selenide (PbSe) and Lead Telluride materials are of specific significance with in the field of solar cells and infrared applications [19-22]. A mixer of Pb_S and Bi_2S_3 could stimulate another compound with improved optoelectronic properties, showing promise for use in the solar energy gadgets for the future generation.

In the present study, we examined the compound $PbBiS_2$ as thin films of Lead nitrate, Bismuth nitrate powder and chitosan (CS) polymer by chemical bath deposition and explored its potential application for environmentally friendly energy devices. We confirmed that the mixture of bismuth chalcogenide and Lead chalcogenide could potentially create another harmless protective layer for solar cell applications.

2 Experimental details

2.1. Chemicals

Bismuth nitrate ($Bi(NO_3)_3.5H_2O$), Lead nitrate ($Pb(NO_3)_2$), Ethylenediamine tetraacetic acid (EDTA) and Sodium Thiosulfate ($Na_2S_2O_3$) were purchased from Merck private limited. The chemicals and solvents used above were analytical grade and did not require further purification. Glass substrates (1mm thick) were purchased in the area.

2.2. Preparation of thin films

In a 200 ml glass beaker, first 0.5 g of chitosan polymer was dissolved in 5% acetic acid solution separately. In second 0.125M $Pb(NO_3)_2$ solutions were added to 0.2M $Bi(NO_3)_3.5H_2O$ solution, then 25 ml EDTA and 0.2M $Na_2S_2O_3$ solution was gradually added with continual stirring for the deposition of $PbBiS_2$ thin films. When the solution was stirred, it turned bright yellow. After 30 minutes, it morphed into a dark brown colour. In the reaction bath, the cleaned glass substrates were immersed vertically. For a total of 10.5 hours, film deposition was carried out at three distinct temperatures (600, 700, and 800 Celsius).

2.3. Fabrication of Charge-Discharge

A mixture of 80 wt% of the materials, 10 wt% of acetylene black and 10 wt% of polyvinylidene difluoride (PVdF) as a binder with a weight ratio of 80:10:10 were sufficiently mixed in 3 ml of N-methyl-2-pyrrolidone (NMP) solvent as a paste. This paste was coated onto the stainless steel ($1cm^2$) electrode and dried in an oven at 110°C for overnight before the electrochemical test. This served as the working electrode. Three electrode cell systems were used to evaluate the electrochemical performance by electrochemical impedance spectroscopy (EIS), cyclic voltammetry (CV) and galvanostatic charge-discharge techniques (Autolab-BSTR 10A) at

room temperature. The electrolyte was used as a 0.2 M H_2SO_4 aqueous solution. A platinum and saturated calomel electrode (SCE) was used as a counter and reference electrodes, respectively.

2.4. Sample characterization

X-ray diffraction was used to examine the samples crystalline structures (XRD). A scanning electron microscope (SEM) with an energy dispersive analysis of X-ray (EDAX) analyzer was used to evaluate the surface morphology and elemental composition of films. The resulting films optoelectronic properties were measured using a double beam spectrophotometer. The sample's conductivity was determined, and Hall parameters such as Hall coefficient, Mobility, and carrier concentration were estimated using a Hall measurement instrument. A spectrofluorometer was used to analyse the samples for photo luminescence. The samples current-voltage characteristics were measured using a two-probe approach with an electrometer at room temperature. The slope of I-V characteristics is used to compute electrical parameters.

3. Results and discussion

Fig. 1. shows the XRD pattern of CS-$PbBiS_2$ thin films deposited at different deposition temperatures (60^0C,70^0C and 80^0C). The films are discovered to be polycrystalline and orthorhombic in structure [21]. With varied deposition temperatures, the projected grain size and strain are shown in the Fig. 2. It means that at 70°C, high-quality films with maximum thickness may be made. At high temperatures (over 70°C), there was also a decrease in grain size as strain increased. This is owing to some Pb and Bi atoms re-evaporating at high temperatures. The intensity of peak (101) increases substantially faster than that of other peaks (301), (270), and (022), showing that the (101) plane is a relatively preferred structural orientation. Peaks (101), (301), (270), and (022) are stated to be characteristic peaks for $PbBiS_2$ thin films, and they match normal JCPDS data well (73-1939). For the three films, the orientations of all peaks have been examined. The preferred orientation of $PbBiS_2$ thin films is found to be along the (101) plane.

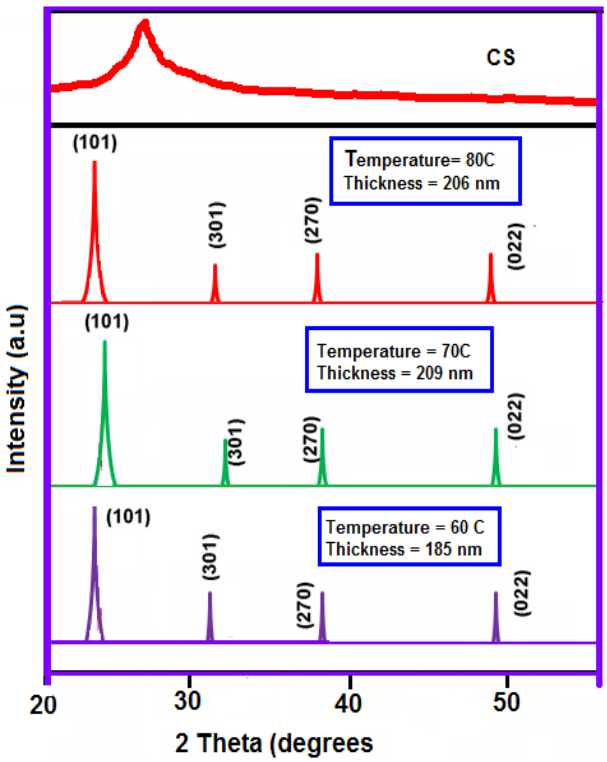

Fig. 1. XRD patterns of CS-$PbBiS_2$ thin films at different deposition temperatures.

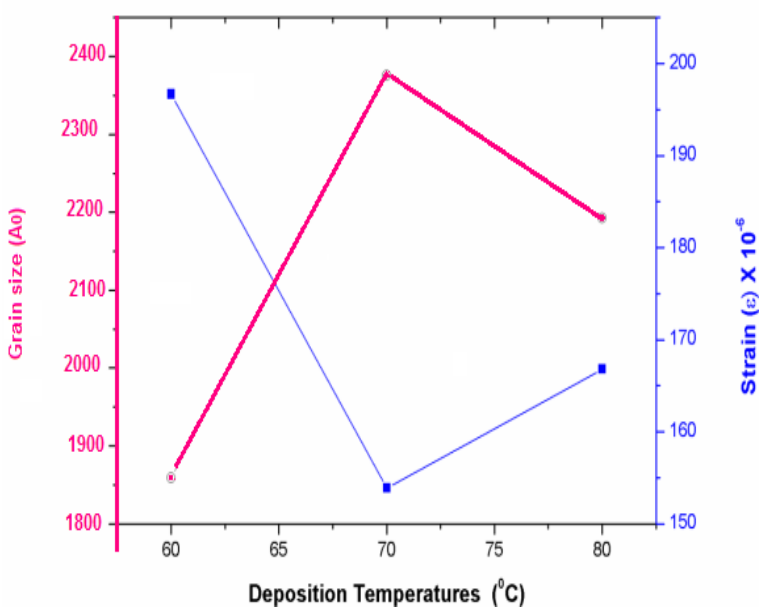

Fig. 2. Variation of grain size and strain with different deposition temperatures.

Fig. 3. displays the EDAX Spectra of $PbBiS_2$ thin films deposition for 10.5 hours at optimum temperature (70°C). It was discovered that the average atomic percentage of Pb:Bi:S ($PbBiS_2$) is virtually stoichiometric in each case without any other impurities. Pb:Bi:S growth is confirmed with thickness at the optimum temperature (70°C). The surface morphology of films with highly reflective surfaces and metallic appearance is shown in Fig. 4.1-4.3. On the substrates, the films grow in a homogenous and uniform manner [22].

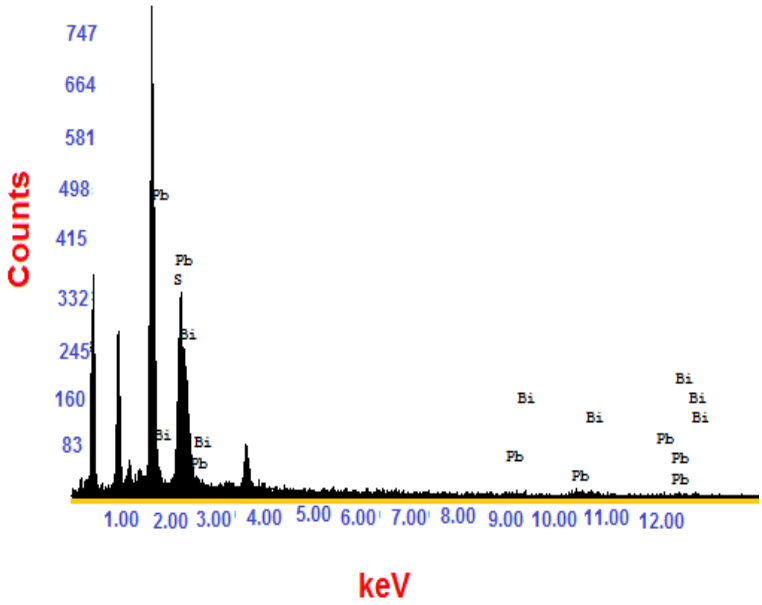

Fig. 3. EDAX Spectra of CS-$PbBiS_2$ thin films at optimum temperature (70©).

The absorption and transmittance spectra of $PbBiS_2$ thin films for various deposition temperatures are shown in Fig. 5, and the material is shown to be highly absorbent in nature with transmittance decreasing with increasing deposition temperatures up to the optimal level (70°C). This improvement can be attributed to the films perfection and stoichiometry [18].

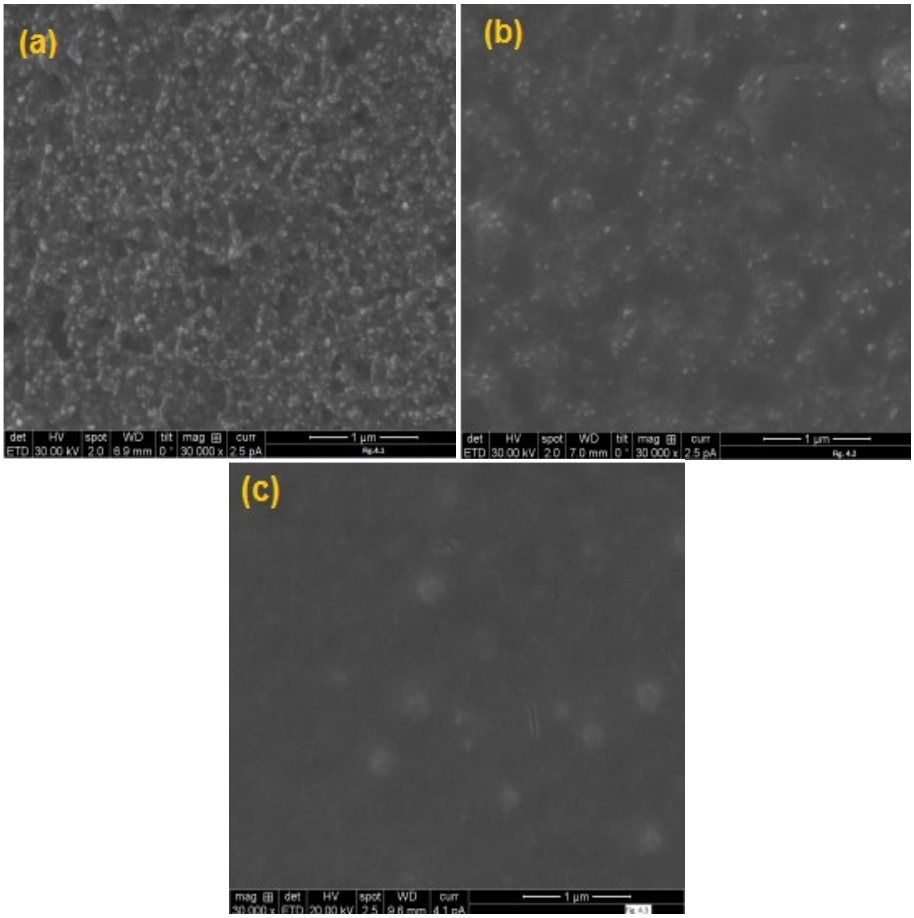

Fig. 4. SEM of CS-PbBiS_2 thin films deposited for different deposition temperatures (60℃, 70℃ & 80℃).

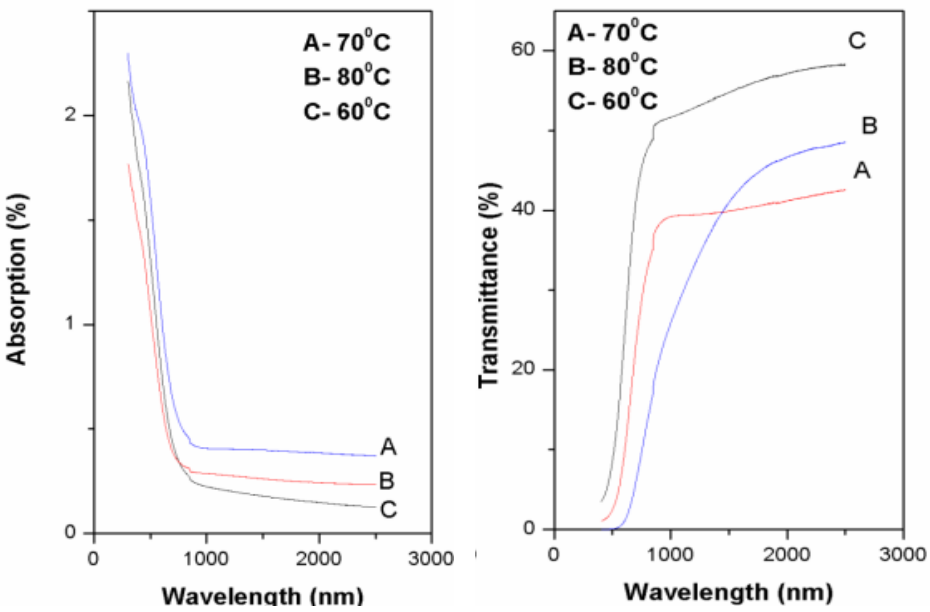

Fig. 5. Absorption and transmittance spectra of CS-PbBiS_2 thin film.

In Fig. 6, the optical band gap reduces as the deposition temperature rises (up to 70°C). Increase the deposition temperature to 80°C and, more importantly, due to adatom mobility, the band gap (Eg) energy value increases dramatically, resulting in increased crystalline size and crystallinity of the films. This behavior is also visible, and it is attributed to the etching process, which takes place at a temperature greater than the optimum. Quantum confinement effect in films is suggested by the decrease in band gap and increase in crystallinity as a function of film thickness. In other words, the variation is attributed to very small crystallites that make up a thin film, resulting in charge carrier quantum confinement in the crystallites [20]. Fig. 7 depicts the optical band gap and thickness of films made at various deposition temperatures. The Hall Studies, which are shown in Fig. 8, are used to determine the various electrical parameters of the $PbBiS_2$ thin films. The values of the Hall coefficients show that $PbBiS_2$ is an n-type semiconductor [21].

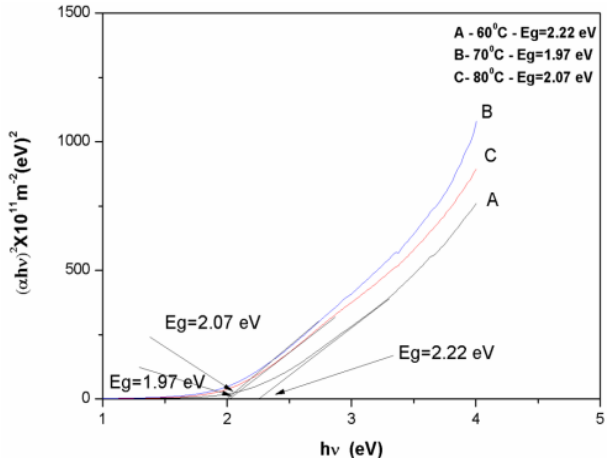

Fig. 6. hv Vs $(\alpha hv)^2$ of CS-$PbBiS_2$ thin films of different deposition temperatures.

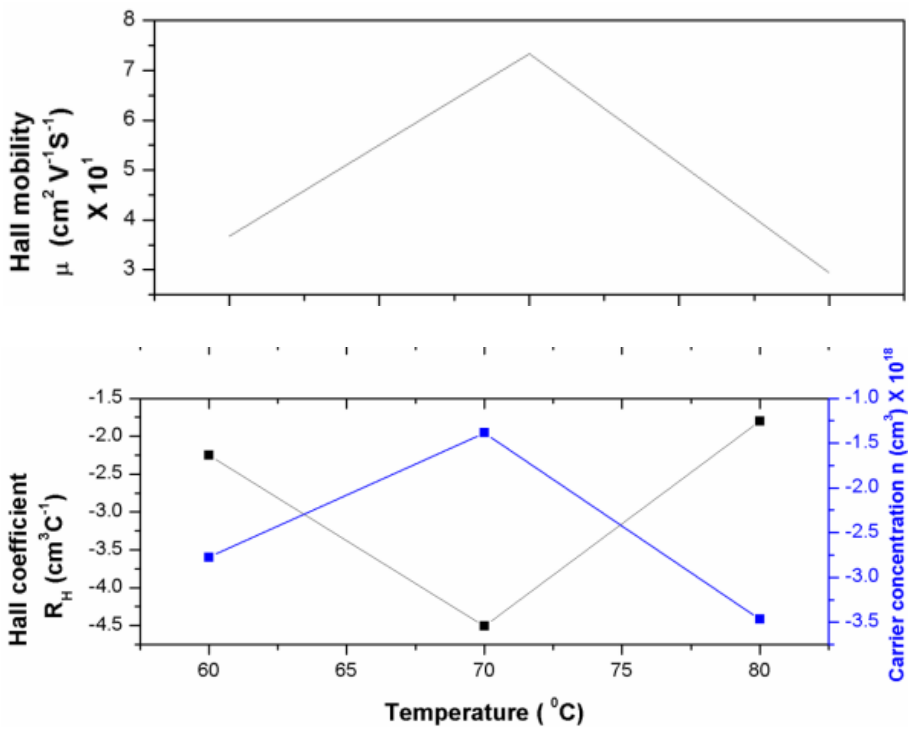

Fig. 7. Variation of optical band gap and thickness of films with different deposition temperatures.

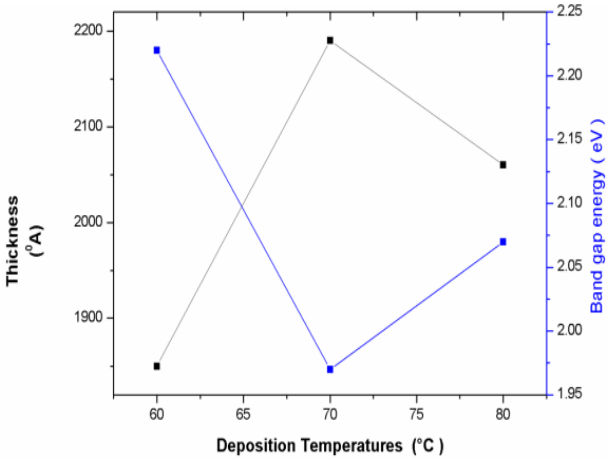

Fig. 8. Variation of Hall parameters with different deposition temperatures.

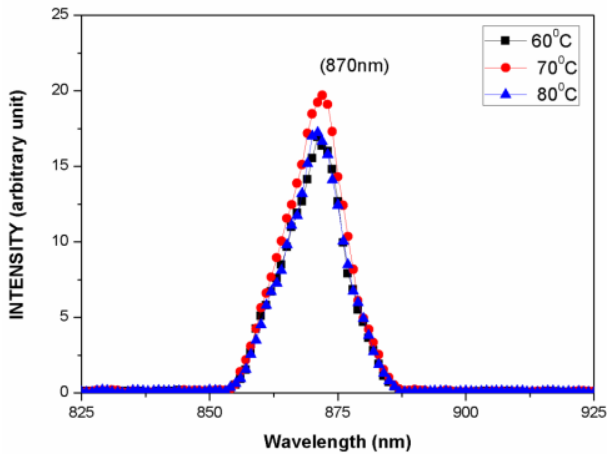

Fig. 9.Photoluminescence emission spectra of $PbBiS_2$ thin films for different deposition temperatures.

The Hall coefficient and mobility increase as the temperature rises. However, as the temperature rises (to 80°C), the Hall coefficient and mobility decrease due to re-evaporation of atoms. Increased deposition temperatures (up to 70°C) cause a decrease in carrier concentration and, as a result, an increase in Hall mobility in the films. As shown in the structures of these film samples, this can be explained by an increase in grain size and a decrease in flaws. Furthermore, the tendency of increasing mobility with decreasing carrier concentration can be attributed to charge carrier scattering at grain boundaries in polycrystalline films. The decrease in mobility at higher temperatures is due to charge carrier lattice scattering. Furthermore, a high carrier concentration implies a reduction in mobility. The fact that the Hall coefficients are negative suggests that the bulk of charge carriers in chemical bath formed $PbBiS_2$ thin films are electrons.

The emission and excitation spectra of $PbBiS_2$ thin films produced at various deposition temperatures with 0.125 M lead nitrate concentration are shown in Fig. 9 and Fig.10. When the material is excited by 580 nm, a sharp and narrow emission peak at 870 nm is found, indicating non-trap related emission. Peak intensities are reported to rise with higher deposition temperatures. At 70°C, the relative intensity is deemed high. The intensity of the $PbBiS_2$ spectrum drops at a deposition temperature of 80°C, which can be attributed to re-evaporation Pb atoms [19] and confirmed by XRD analysis.

The films PL emission intensity is greatly influenced by particle size and shape. Because of the enhanced crystallinity of the films, the luminescence increases as the temperature rises (up to 70°C). The peak intensity of greater-thickness films (at 70°C) is significantly higher than that of lower-thickness films. This may be the result of the shape effect. The PL intensity is influenced by

the form of the materials. All of the emissions are linked to defects that appeared during crystallite growth and are related to crystallinity deformation caused by dislocations and big vacancies. The peak emission wavelength always shifts to the right. When compared to the peaks of the excitation spectra, the peak emission wavelength invariably changes towards the long wavelength of the spectrum.

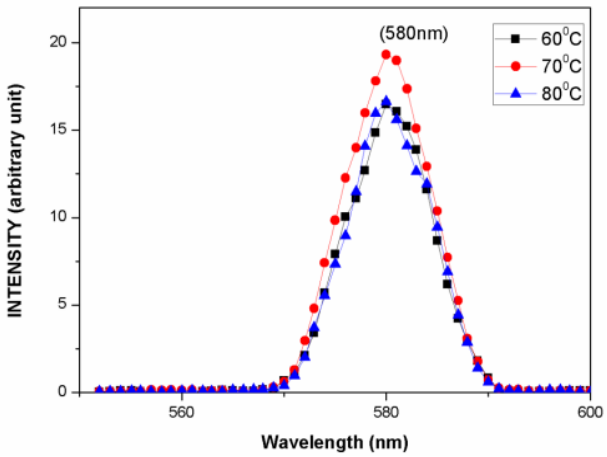

Fig. 10. Photoluminescence excitation spectra of CS-PbBiS$_2$ thin films for different deposition temperatures.

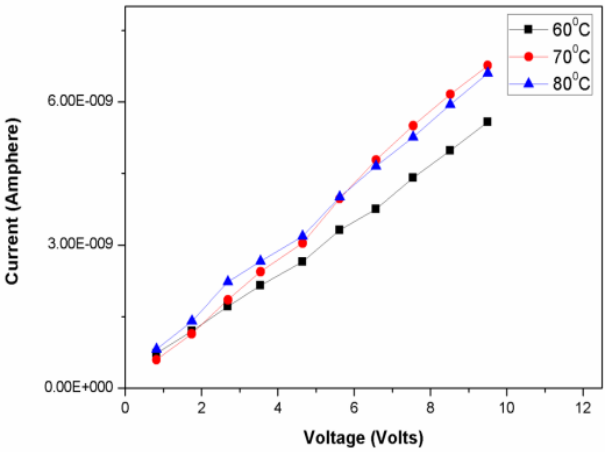

Fig. 11. Current - voltage plot of CS-PbBiS$_2$ films for different deposition temperatures.

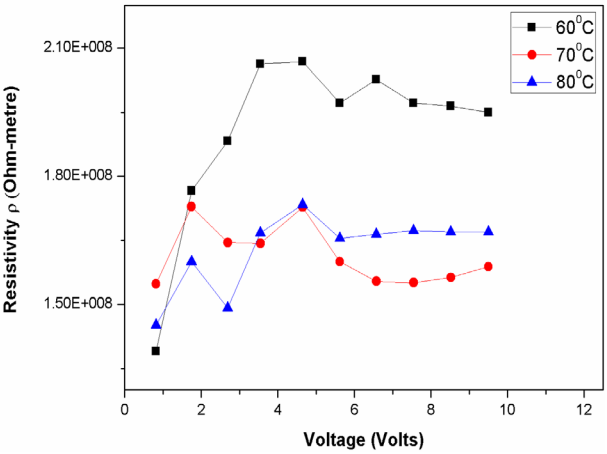

Fig. 12. Resistivity - voltage plot of CS-PbBiS2 films for different deposition temperatures.

The Stokes shift is the name for this occurrence. As a result, these films find commercial use in luminous gadgets. Current fluctuates with applied voltage, as shown in Fig.11 and Fig.12. Film conductivity rises with temperature until it reaches 70°C, then falls. Resistivity increases at higher temperatures (80°C) due to a decrease in layer thickness. The films high resistivity could be owing to its high grain boundary density, discontinuities, and thin thickness [18]. The semiconducting characteristic of film is demonstrated by the fact that resistivity reduces as temperature rises.

4. Conclusions

Thin films of CS-$PbBiS_2$ produced via CBD were studied. The films have a crystalline character with an orthorhombic structure, according to XRD measurements. According to our findings, the grain size of the resulting films was enhanced to an optimal level. The average atomic percentage of Pb:Bi:S demonstrates roughly the stoichiometric composition, according to EDAX analysis. The findings of SEM analysis revealed that all of the films have a highly reflective surface with a metallic appearance. Optical investigations found that when layer thickness increased, the band gap value decreased. Furthermore, the $PbBiS_2$ films reduced transmittance and higher absorption values in the visible and near-infrared regions showed that they might be employed as an absorber layer in thin film solar cells.

The thin films I-V characteristics indicated their semiconducting nature, which has advantages for photovoltaic's. The negative character of the Hall coefficient suggests that electrons make up the bulk of charge carriers, according to the Hall Effect research. The intensity of the emission increases with the thickness of the coatings, according to a PL investigation. When compared to the peaks of excitation spectra, the peak emission wavelength invariably changes towards the long wavelength of the spectrum. As a result, these films find commercial use in luminous gadgets. $PbBiS_2$ films have good features that make them promising materials for enhancing the activity of semiconductors for photoelectric conversions, allowing them to be used directly in optoelectronic and photovoltaic devices.

References

[1] Srimathy N and Kumar A R 2016 Superlattices and Microstructures Structural and optical characterization of thermally evaporated bismuth and antimony films for photovoltaic applications J.Superlatt.microstru. 93 1; https://doi.org/10.1016/j.spmi.2016.02.026

[2] Kim Y, Yang Z, Jain A, Voznyy O, Kim G, Liu M, Quan L N, De Arquer F P G, Comin R, Fan J Z and Sargent E H 2016 Pure Cubic-Phase Hybrid Iodobismuthates AgBi2I7 for Thin-Film J.Photovol. 128 1; https://doi.org/10.1002/ange.201603608

[3] Kim K S, Zhao Y, Jang H, Lee S Y, Kim J M, Kim K S, Ahn J, Kim P, Choi J and Hong B H 2008 Large-scale pattern growth of graphene films for stretchable transparent electrodes Nature 457 706; https://doi.org/10.1038/nature07719

[4] Guo W, Zhang M, Banerjee A and Bhattacharya P 2010 Catalyst-free InGaN/GaN nanowire light emitting diodes grown on (001) silicon by molecular beam epitaxy Nano Lett. 10 3355; https://doi.org/10.1021/nl101027x

[5] Zhao W, Ribeiro R and Eda M 2015 Electronic structure and optical signatures of semiconducting transition metal dichalcogenide nanosheets Acc. Chem. Res. 48 91; https://doi.org/10.1021/ar500303m

[6] Ali N, Hussain A, Ahmed R, Wan Shamsuri W N and Fu Y Q 2016 Synthesis and characterization of copper antimony tin sulphide thin films for solar cell applications, Appli. Surf. Sci. 390 393; https://doi.org/10.1016/j.apsusc.2016.08.136

[7] Gielis J J H, Gevers P M, Aarts I M P, Van De Sanden M C M and Kessels W M M 2014 Optical second-harmonic generation in thin film systems Optical second-harmonic generation in thin film systems Plasma and Mat. Processing. 26 1519; https://doi.org/10.1116/1.2990854

[8] Brandt R E, Kurchin R C, Hoye R L Z, Poindexter J R, Wilson M W B, Sulekar S, Lenahan F, Yen P X T, Stevanovi V, Nino J C and Bawendi M G, Buonassisi T 2015 Investigation of Bismuth Triiodide (BiI3) for Photovoltaic Applications J. Phy. Chem. Lett. 6 4297; https://doi.org/10.1021/acs.jpclett.5b02022

[9] Kulkarni S S and Lokhande C D 2003 Structural, optical, electrical and dielectrical properties of electrosynthesized nanocrystalline iron oxide thin films Mater. Chem. Phys. 82 151; https://doi.org/10.1016/S0254-0584(03)00212-8

[10] Rahman M A and Khan M K R 2014 Materials Science in Semiconductor Processing Effect of annealing temperature on structural , electrical and optical properties of spray pyrolytic nanocrystalline CdO thin films Mater Sci. Semicond. Process. 24 26; https://doi.org/10.1016/j.mssp.2014.03.002

[11] Herrero J and Guille C 2010 Optical , electrical and structural characteristics of Al : ZnO thin films with various thicknesses deposited by DC sputtering at room temperature and annealed in air or vacuum Vaccum. 84 924; https://doi.org/10.1016/j.vacuum.2009.12.015

[12] Pentia E, Pintilie L, Matei I, Botila T and Pintilie I 2003 Combined chemical-physical methods for enhancing IR photoconductive properties of PbS thin films, Infrared Phys. Technol. 44 207; https://doi.org/10.1016/S1350-4495(02)00225-6

[13] Wei X D, Cai C F, Zhang B P, Hu L, Wu H Z, Zhang Y G, Feng J W, Lin J M, Lin C, Fang W Z and Dai N 2011 PbTe photovoltaic mid-IR detectors, J. Infrared Milli. Waves.30 293; https://doi.org/10.3724/SP.J.1010.2011.00293

[14] Gertman R, Osherov A, Golan Y and Visoly-Fisher I 2014 Chemical bath deposited PbS thin films on ZnO nanowires for photovoltaic applications, Thin Solid Films. 550 149; https://doi.org/10.1016/j.tsf.2013.10.160

[15] Acharya K.P, Hewa-Kasakarage N N, Alabi T R, Nemitz I, Khon E, Ullrich B, Anzenbacher P and Zamkov M 2010 Synthesis of PbS/TiO 2 Colloidal Heterostructures for Photovoltaic Applications, J. Phys. Chem. C 114 12496; https://doi.org/10.1021/jp104197s

[16] Fu L and Yu M 2014 Carbon Nanotubes Based Thin Films: Fabrication, Characterization and Applications Rev. Adv. Mater. Sci. 36 40.

[17] Balasubramanian V and Suriyanarayanan N 2013 Preparation and characterization of novel single-crystalline PbBiS2 thin films, Mater. Lett. 91 362; https://doi.org/10.1016/j.matlet.2012.09.099

[18] Mane R S and Lokhande C D 2000 Chemical deposition method for metal chalcogenide thin films Mater. Chem. Phys. 65 1; https://doi.org/10.1016/S0254-0584(00)00217-0

[19] Czaban J A, Thompson D A and LaPierre R R 2008 GaAs core- shell nanowires for photovoltaic applications Nano Lett. 9 148; https://doi.org/10.1021/nl802700u

[20] Chopra K L, Paulson P D and Dutta V 2004 Thin-film solar cells: an overview, Prog. Photovolt. Res. Appl. 12 69; https://doi.org/10.1002/pip.541

[21] Castro M V and Tavares C J 2015 Dependence of Ga-doped ZnO thin film properties on different sputtering process parameters: Substrate temperature, sputtering pressure and bias voltage, Thin Solid Films. 586 13; https://doi.org/10.1016/j.tsf.2015.04.036

[22] Perednis D and Gauckler L J 2005 Thin film deposition using spray pyrolysis, J. Electroceramics 14 103; https://doi.org/10.1007/s10832-005-0870-x